EngOpt 2008 - International Conference on Engineering Optimization
Rio de Janeiro, Brazil, 01 - 05 June 2008.

Optimization of Piezoelectric Actuators for Manipulators with Flexible Non-prismatic Links

Valdecir Bottega‡ **Rejane Pergher**‡ **Alexandre Molter**† **Jun S. O. Fonseca**†
vbottega@ucs.br rpergher@ucs.br alexandremolter@bol.com.br jun@ufrgs.br

‡ UCS - Universidade de Caxias do Sul, Dep. Mathematics and Statistics
R. Francisco Getúlio Vargas, 1130, 95570-560, Caxias do Sul, RS - Brazil

† UFRGS -Universidade Federal do Rio Grande do Sul, Dep. Mechanical Engineering
R. Sarmento Leite, 425, 90050-170, Porto Alegre, RS – Brazil

1. Abstract

This work presents a tracking control model for a flexible robotic manipulator using motor torques and piezoelectric actuators. The dynamic model of the flexible manipulator is obtained in a closed form through the Lagrange Eq.s. The control uses the motor torques for the joints tracking control and also to reduce the low frequency vibration induced in the manipulator links. The stability of this control is guaranteed by the Lyapunov stability theory. Piezoelectric actuators and sensors are added for vibrations with frequencies beyond the reach of motor torque control.

Robots' flexible links are built in complex geometries, which cannot be modeled by simple beam bending Eq.s. In this work we propose a methodology for accounting the complex geometry within the realm of the Euler-Bernoulli beam theory. The natural frequencies are calculated by the finite element method and the approximated eigenfunctions are interpolated by polynomials. Three mdes are used for the dynamics of the arm, while only two modes are used for the control. Additionally, this work introduces a formulation for simultaneous optimization of control and actuators and sensors through of dissipated energy maximization in the system by the control action with location and sizing optimization of piezoelectric actuators and sensors in the structures. Numerical experiments on Matlab/Simulink are used to verify the efficiency of the control model.

2. Keywords: *Piezoelectric actuators, flexible links, tracking control, optimization, manipulators.*

3. Introduction

The need of lightweight robots has attracted the attention of researchers everywhere to robotic manipulators with flexible links. These robots are essential in mobile applications, such as surface vehicles, aircrafts, and spacecrafts. The design of these manipulators requires a control system, which takes into account the interaction of the joint angles and the elastic modes. This complex task has the additional complication of the essential uncertainty that characterizes robotic manipulators, such as variable payload and joint frictional torques [1].

A flexible robot control design is composed by two steps: a robust tracking control, acting on the joint angles, and a stabilizer for the motion induced vibration suppression. Robotic systems can be considered linear in relation to some parameters, as mass, inertia, and damping factors, but this assumption is not valid for the state. Therefore, a position control law must be defined with an appropriate tracking error assymptotic stability, obtained with Lyapunov functions [2].

A stabilizer to damp the elastic oscillation is designed based on a linearized model. However, the high frequency modes cannot be eliminated by the motor torque action alone, because their period is smaller than the torque control system can handle. Thus, the control of those vibrations must use higher frequency actuators like piezoelectrics.

Robots' flexible links are built in complex geometries, which cannot be modeled by simple beam bending Eq.s. In this work we propose a methodology for accounting the complex geometry within the realm of the Euler-Bernoulli beam theory.

The used of finite elements method for the determination of the eigenvectors is necessary since the analytical approach is cumbersome for complex non-prismatic beams. However, since we wish to retain the simplicity of the analytic derivation of the control, the eigenvectors are interpolated from the nodal values with polynomials [3]. The effectiveness of this interpolation is checked by the Rayleigh quotient [4].

In this work we propose a tracking control model for a robot arm with flexible links, where the motor torque controls the joint angle tracking and reduce the low frequency vibrations on the links. Piezoelectric sensors and actuators are added to control the high frequency vibrations beyond the torque control. In the simulations it was used three modes and in the control two modes were used. A Matlab/Simulink code was created to assess the control model efficiency.

4. Dynamic Model

The physical system considered in this work is composed by a rigid and a flexible link, joints and motors, it is based on the robot design suggested by Bottega [5], but the geometry was generalized to allow non-prismatic designs. The second link was considered flexible and non-prismatic, therefore subject to motion induced vibration, which affect the trajectory of the endpoint. The sketch of a possible non-prismatic flexible link is shown in Figure 1. This link has a linearly varying cross section.

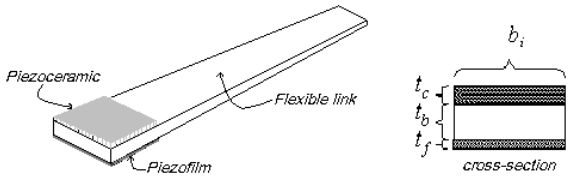

Figure 1. Link non-prismatic and flexible.

The motion of the robot endpoint is a composition of the successive relative link motions. This movement is described using homogeneous matrix transformations. These transformations represent translations and rotations due to the joints angle change and the flexible link elastic deflections [6]. The deflections are obtained considering each link as a uniform beam with a_i length featuring a piezoceramic actuator bonded to the top face and piezofilm sensor bonded to the bottom face, as shown Figure 1. Links are modeled as Euler-Bernoulli beams, with deflection dyi(x_i,t) satisfying the partial differential equation

$$(EI)_i \frac{\partial^4 d_{yi}(x_i,t)}{\partial x^4} + \rho_i \frac{\partial^2 d_{yi}(x_i,t)}{\partial t^2} = 0, \tag{1}$$

where ρ_i is the uniform density and (*EI*)*i* is the flexural rigidity constant of the link [7].

Exploring the time and space separability on Eq.(1) by the modal analysis technique, the link deflection can be expressed as

$$d_{yi}(x_i,t) = \sum_{i=1}^{m_i} \varphi_{ij}(x_i)\delta_{ij}(t), \tag{2}$$

where each term in the general solution of Eq.(1) is the product of a time harmonic function of the term $\delta_{ij}(t) = e^{j\omega_{ij}t}$ and of a space eigenfunction of the form

$$\varphi_{ij}(x_i) = C_{1ij}\sin\left(\frac{\rho_i\omega_{ij}^2}{(EI)_i}x_i\right) + C_{2ij}\cos\left(\frac{\rho_i\omega_{ij}^2}{(EI)_i}x_i\right) + C_{3ij}\sinh\left(\frac{\rho_i\omega_{ij}^2}{(EI)_i}x_i\right) + C_{4ij}\cosh\left(\frac{\rho_i\omega_{ij}^2}{(EI)_i}x_i\right), \tag{3}$$

where ω_{ij} is the *j*th natural angular frequency of the eigenvalue problem for link *i*. The determination of the constant coefficients *Ckij* uses clamped conditions at the link base and mass boundary conditions representing the balance of bending moment and shearing force at the link endpoint [8].

This solution is possible when the link geometry is prismatic or slightly non-prismatic. If the link shape is irregular it is very difficult to obtain a closed form analytic solution. It is important to generalize the approach for other link shapes.

5. Approximating solutions for eigenfunctions

The links of the mechanic manipulators are modeled as beams, since their lengths are much larger than the cross-sectional height depth. Thereby, considering that the control can prevent large displacements, it is possible to apply the Euler-Bernoulli theory for a small displacements, where the equilibrium solution is given by

$$\int_0^l \frac{d^2}{dx^2}\left(EI\frac{d^2 d_y(x)}{dx^2}\right)dx - \int_0^l p(x)dx = 0,\ 0 \le x \le l, \tag{4}$$

where *p(x)* are external forces actuating on the beam.

For small displacements, the natural frequencies and modes can be considered independent of the external forces. Using the finite element method, it is possible to define [3] the mass, stiffness and damping matrices, respectively, by

$$K_{ij} = \int_0^L EI\frac{d^2\psi_i}{dx^2}\frac{d^2\psi_j}{dx^2}dx \tag{5}$$

$$M_{ij} = \int_0^L \rho d\psi_i d\psi_j dx, \tag{6}$$

$$C = \alpha M + \beta K, \tag{7}$$

where ψ are the elementwise interpolation functions and α, β are the Rayleigh damping constants. Usually four cubic Hermite polynomials are as interpolation functions in each two-node finite element so the unknowns of the approximated problem are nodal displacements and its derivatives. The mass matrix can be further approximated by its lumped (diagonal) form. Then the natural modes and frequencies can be computed by the following eigenvalue problem

$$\left|K - \omega^2 M\right| = 0, \tag{8}$$

where ω^2 are the characteristic values from the Eq.(8). The eigenvectors represent the vibration modes in nodal coordinates.

Considering that the control algorithm requires twice differentiable eigenfunctions, it is necessary to create a continuous interpolation from the discrete values. The natural choice would be using the same elementwise Hermite polynomials used by the finite element approximation, but the eigenfunctions φ presents big oscillations, due to excessive sensitivity to the numerical imprecision, specially of the derivatives. Figure 2 shows these oscillations for the first and second mass-normalized eigenfunction interpolation.

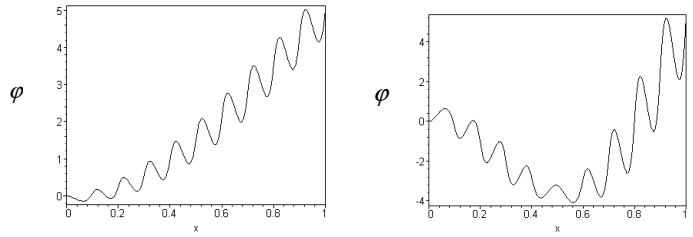

(a) ***(b)***

Figure 2. Eigenfunctions which represent the vibration modes of a link fixed on *x=0* . *(a)* it is the first mode and *(b)* the second mode. Eigenfunctions generate through the interpolation with Hermite polynomial in each element.

It is possible to smooth these disturbances by choosing another set of interpolation functions. In this case, we chose to forgo the elementwise Hermite approximation for a global interpolation ignoring the derivatives of the inner nodes. Three alternatives are considered: interpolating all nodes with a single Hermite approximation, a mixed Hermite-Lagrange set of polynomials which satisfies the displacements and derivatives at the outermost nodes, but only the displacements at the inner nodes, and finally a least-squares polynomial regression.

For computing the coefficients by least-squares it is necessary to considerate the pseudoinverse operator A^+ [9]. This operator has the following properties: if A^TA is invertible, then $A^+ = \left(A^TA\right)^{-1}A^T$; if AA^T is invertible, then $A^+ = A^T\left(AA^T\right)^{-1}$. The coefficients from the polynomials are calculated from the results of the linear system $Ax = y$, hence $x = A^+ y$.

The matrix *A* comes from the mesh of finite element and *y* from the eigenvectors values and they are calculated from

$$A = \begin{bmatrix} x_1^n & \cdots & x_1^1 & 1 \\ x_2^n & \cdots & x_2^1 & 1 \\ \vdots & \cdots & \vdots & \vdots \\ x_i^n & \cdots & x_i^1 & 1 \end{bmatrix}, \quad y = \begin{bmatrix} y_1 \\ y_2 \\ \vdots \\ y_i \end{bmatrix}, \tag{9}$$

where *n* is the order of the polynomials and *i* is the number of points at the mesh.

All there three options can eliminate the oscillations on the eigenfunctions, but might be inadequate for use in the control solution, since the differentiation and the integration can generate different results. For this way, it is interesting adopt an error criterion. In this work it is adopted the Rayleigh Quotient as error criterion [4], which for analytic functions can be expressed from

$$\omega^2 = \frac{\int_0^l EI\left(\frac{d^2\varphi}{dx^2}\right)^2 dx}{\int_0^l \rho a \varphi^2 dx}, \tag{10}$$

where *a* is the cross-section from the link. The discrete form is given by $\omega^2 = \frac{\varphi^T K \varphi}{\varphi^T M \varphi}$, where in this case φ are the eigenvectors.

In this work we have tested the three approximation schemes proposed. Results show that they can eliminate oscillations, but with different effect on the Rayleigh Quotient. Figure 3 shows the smoothed resulting mode shape, free from the oscillations for the mixed Lagrange-Hermite formulation.

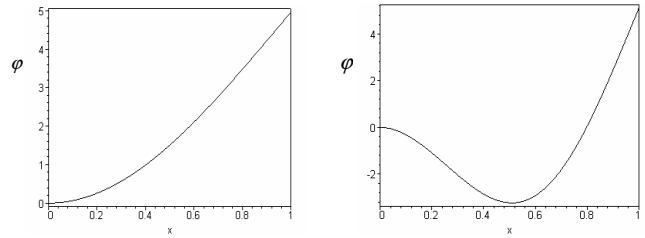

(a) *(b)*

Figure 3. Eigenfunctions which represent the vibration modes of a link fixed on *x=0*. *(a)* it is the first mode and *(b)* the second mode. Eigenfunctions generate through the interpolation with mixed Lagrange-Hermite polynomials.

The eigenvalue error of the smoothed eigenvectors in Eq.(10) and the original eigenvalues from the Eq.(8) are around 1Hz for the first and the second mode and 2Hz for the third mode, which means around 5% for the first vibration mode and smaller for the second and third.

For geometric complex links, the complete Hermite approximation gives smaller eigenfunctions errors.

6. Equations of motion

The closed form equations of motion are derived using a Lagrangian approach, in the form of compact matrices, resulting [6]

$$B(q)\ddot{q} + C(q,\dot{q})\dot{q} + Kq + D\dot{q} + g(q) = u \tag{11}$$

where $q = [\theta, \delta]^T$ is the generalized coordinates vector, θ is the *nx1* joint coordinates vector, δ is the *nx1* elastic modes coordinates vector, *B(q)* is the positive definite symmetric inertia matrix, $C(q,\dot{q})$ is the Coriolis and centrifugal forces vector, *g(q)* is the gravitational torque vector, *K* is the positive definite stiffness diagonal matrix, *D* is the positive semidefinite link diagonal damping matrix and *u* is the joint input torque vector.

The *K* matrix is calculate directly by the finite element method and can be diagonalizable by the eigenvalues from the Eq.(8) on the main diagonal.

The values from δ represent the amplitudes from the vibration modes and can be calculated from the equation of minimum potential energy:

$$[\delta_i]^T \left[\int_0^l EI \left(\frac{d\varphi_i d\varphi_j}{dx^2} \right)^2 dx \right] [\beta_i] - [p_i]^T [\beta_i] = 0, \forall \beta_i, i, j = 1,2,..,n \tag{12}$$

where p_i are the forces apply about the link, *n* is the number of eigenfunctions φ, calculated according to showed above and β_i are virtual amplitudes introduced in the equation which can assumed any value.

7. Tracking control

This section introduces the flexible robot arm tracking control, based on an adaptive controller and a robust control law to reduce the elastic vibrations of the arms. The improved tracking controller using nominal compensation of dynamic nonlinearities of system Eq.(11) is given by

$$u = B(q)\ddot{q}_r + C(q,\dot{q})\dot{q}_r + K\, q_d + D\dot{q}_r + g(q) - K_p s \tag{13}$$

where K_p is the positive definite diagonal gain matrix, $\dot{q}_r = \dot{q} - \Lambda\tilde{q}$ is the reference velocity vector, with tracking error $\tilde{q} = q - q_d$, q is the robot path, q_d is the desired path and $s = \dot{q}_d - \dot{q}_r = \dot{\tilde{q}} + \Lambda\tilde{q}$ is the reference error.

We can prove using Lyapunov stability theory [11] that with control law (13) the tracking error tend to zero and the deflection modes remain bounded. However, the damping may be too small. In this case, we can add a control law $D'_\Delta \dot{\delta}_d$, depend on tracking dynamics obtained from the q_d variable:

$$D'_\Delta \equiv D_\Delta - diag\{f_{11},..., f_{nn}\} \tag{14}$$

where D_Δ is the positive definite diagonal gain matrix and f_{ij} are functions that depend on the deflection velocities.

The Eq. (14) is added to Eq.(13) to obtain the control law of the system Eq.(11) expressed as

$$u = B(q)\ddot{q}_r + C(q,\dot{q})\dot{q} + K_e q_d + D\dot{q}_r + g(q) - K_p s + \left[0^T \left(D^{'}\Delta\dot{\delta}_d\right)\right]^T \tag{15}$$

where $D_\Delta^{'}\dot{\delta}_d$ is a robust control action that damp the system and eliminate the steady vibrations.

8. Vibration control

We propose a feedback control voltage to the piezoceramic actuator [12], expressed as

$$P(t) = -c_a K_c c_a^T \dot{P}_f(t) \tag{16}$$

with

$$c_a = \frac{E_b E_c t_c t_f d_{31}}{\rho_b A_b \left(E_b t_b + 6 E_c t_c\right)} \left(\varphi^{'}\left(x_a + a_{pc}\right) - \varphi^{'}\left(x_a\right)\right), \tag{17}$$

where K_c is the feedback gain, E_c and E_b are the elastic modulus of the piezoceramic and the link, respectively, t_c, t_f and t_b are the piezoceramic, piezofilm, and link thicknesses, respectively, A_b is the cross section of the link, d_{31} is the piezoelectric constant and ρ_b is the mass density, a_{pc} is the size of the actuator, x_a is the localization from the actuator on the link, $\dot{P}_f(t)$ is the voltage generated by the piezofilm sensor, obtained by integrating the electric charge developed at a point on the piezofilm, expressed as:

$$P_f(t) = c_s \delta = \frac{k_{31}^2 b_f}{C g_{31}} d_{ni} \delta \tag{18}$$

where k_{31}^2 is the electromechanical coupling factor, C is the capacitance of the film sensor, d_{ni} is the distance from the bottom of the piezofilm sensor to the neutral axis and g_{31} is the piezoelectric stress constant [13]. This additional controller Eq.(16) is combined to the original one. The resulting control law for the system Eq. (15) is expressed as

$$u = B(q)\ddot{q}_r + C(q,\dot{q})\dot{q} + K q_d + D\dot{q}_r + g(q) - K_p s + \left[0^T \left(D^{'}\Delta\dot{\delta}_d\right) + c_a P(t)\right]^T. \tag{19}$$

Using Lyapunov stability theory on Eq.(19) we can prove that the trajectory and flexible link deflections result assymptotically stable for this control law.

9. Location and sizing actuators optimization

Controlling structural vibration depends not only on the control law, but also on the selection and location of the actuators and sensors [14]. In this work we propose a methodology for the actuator and sensor position and sizing optimization, based on maximizing the control energy dissipation [15]. This procedure takes into account the actuators and sensors mass and stiffness, and their effect on the mechanical behavior of the structure. This influence is combined to the control characteristics to obtain an objective function that depends on the actuators location and sizing and the control gain.

The deflections are obtained considering each link as a beam with a_i length featuring, a piezoceramic actuator bonded to the top face and a piezofilm sensor bonded to the bottom face as shown Figure 1.

The dynamic of the flexible link with m piezoelectric sensors and actuators in terms of modal coordinates can be expressed as

$$B_{\delta\delta}\ddot{\delta}_d + C_\delta \delta_d + K\delta_d + g(\delta) = c_a P(t). \tag{20}$$

The total energy stored in the system [16] can be expressed as

$$W = T + U = \frac{1}{2}\dot{\delta}^T B(\delta)\dot{\delta} + \frac{1}{2}\delta^T K\delta \tag{21}$$

Differentiating the Eq.(21) with respect to the time we obtain

$$W=T+U=\frac{1}{2}\dot{\delta}^T\dot{B}(\delta)\dot{\delta}+\dot{\delta}^T B(\delta)\ddot{\delta}+\delta^T K\delta \ . \tag{22}$$

Using the Eq.(20) and Eq.(22) with the control law Eq.(16), we obtain

$$\dot{W}=\dot{T}+\dot{U}=-\dot{\delta}^T D\dot{\delta}-\dot{\delta}^T(c_a K_c c_a^T c_s)\dot{\delta}<0 \ , \tag{23}$$

where the first and the second terms describe the energy rates removed from the system by the internal damping and by the control feedback, respectively.

Integrating the Eq.(22) we obtain

$$W(t_0)=W_f+W_c=\int_{t_0}^{\infty}\dot{\delta}^T D\dot{\delta}\,dt+\int_{t_0}^{\infty}\dot{\delta}^T(c_a K_c c_a^T c_s)\dot{\delta}\,dt \tag{25}$$

where W_f represent the energies dissipated by internal damping and W_c represent the energies dissipated by the control action.

For effective vibration suppression, it is reasonable to derive a method to increase the energy dissipated by the control. We observe that W_c depends on the locations and the sizing of the actuators and feedback matrix gain K_c . Therefore, W_c can be used as an optimization criterion to determine location and sizing of actuator and feedback gains.

For determining W_c , we write the Eq.(20) in state-space form as

$$\dot{z}=\tilde{H}z \tag{26}$$

where $z=\left[\delta \ , \ \dot{\delta}\right]^T$ and

$$\tilde{H}=\begin{bmatrix} 0 & I \\ -B_{\delta\delta}^{-1}K & -B_{\delta\delta}^{-1}(C_{\delta\delta}+D+c_a K_c c_a^T c_s) \end{bmatrix} \tag{27}$$

The induced control dissipation energy by the active damping control W_c can be written as

$$W_c=\int z^T Qz\,dt \tag{28}$$

where

$$Q=\begin{bmatrix} 0 & 0 \\ 0 & c_a K_c c_a^T c_s \end{bmatrix} \tag{29}$$

it is a $2m\times 2m$ matrix.

Applying standard state transformation techniques to the Eq.(27) we obtain

$$W_c=z_0^T P z_0 \tag{30}$$

where P is symmetric positive definite matrix, solution of the Lyapunov equation

$$\tilde{H}^T P+P\tilde{H}=-Q \tag{31}$$

It is noticeable that W_c depends on the initial conditions of the flexible structure. In order to eliminate this dependence, we assume that initial state of z satisfies $W_a^{-1}z_0$ where $W_a=diag(\lambda_i)$, with random value of $\lambda_i>0$.

Therefore, we obtain an objective function $J_0=tr(W_a P W_a)$ for energy dissipated by the control which depends on the location and the size of the piezoelectric actuators and the gain K_c .

To design a precise and agile manipulator, it is reasonable to take it as light as possible. This is accomplished by adding a function of the actuator and sensor masses to the objective function shown above. We added a quadratic term dependent on the size of the actuator a_{pc} to J_0 [15], resulting in the following composite objective function

$$\begin{aligned} &J_0=\alpha a_{pc}^2-W_c \\ &0\le x_a\le a_i \\ &0<a_{pc}+x_a\le a_i \\ &K_c\le K_{\max} \end{aligned} \tag{32}$$

where α depends on the piezoelectric material cost and $K_{\max}$ depends on the actuator power limitation.

10. Results

This work contains significant improvements with respect to the previously published work [17]. Three vibration modes are used in the simulation, instead of two, while the control is still derived with two modes. The main reason behind this difference is to test if the control is robust enough to damp the additional mode.

The control laws were tested on a simplified model robot with a rigid first link and a flexible second link as shown in Figure 4. Gravitational effects were ignored [18]. The Lagrangean coordinate vector is $q = [\theta_1, \theta_2, \delta_1, \delta_2, \delta_3]^T$.

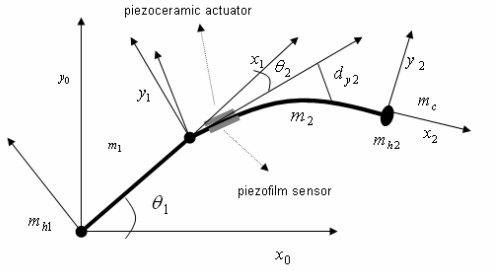

Figure 4. Model of planar one-link flexible manipulator featuring piezoelectric actuators and sensors.

The results were obtained using a block-diagram implemented in MatLab/Simulink, where the fourth-order Runge-Kutta method with $\Delta t = 1$ ms was used to integrate the equations for a five-second simulation.

Figure 5 shows the trapezoidal speed trajectory tracking used with amplitude $\pi/2$ for the joint angles 1 and 2 without initial tracking error.

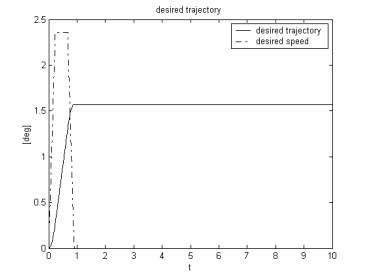

Figure 5. Desired trajectory and speed of the joint angle 1 and 2.

11. Simulations

In this work , we use the mechanical and geometrical properties of the piezoelectric materials presented in [19].

Firstly, we simulated a damped system with a control law, Eq.(13). Figure 6 (a) shows that the elastic deflections tend to zero and they are limited due to natural damping of the system. Figure 6 (b) shows that the system tracking error also tends to zero.

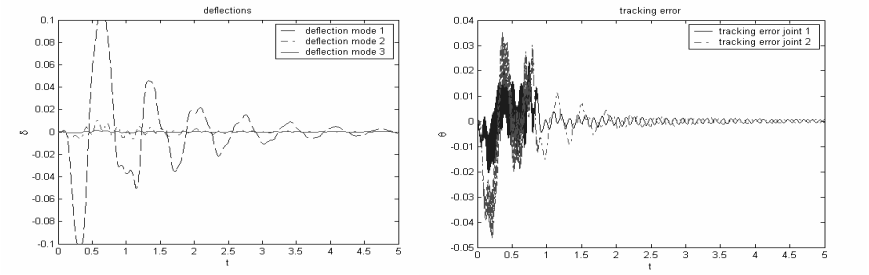

(a) ***(b)***

Figure 6. (a) Deflection of first, second and third modes with damping.(b) Tracking error of the trapezoidal trajectory tracking system.

In the second simulation, we used the control law given by Eq.(17) in the same system used before. Figure 8 (a) shows an increase in the system damping and a zero convergence faster than the deflections. This is a result of the addiction of $D_\Delta \dot{\delta}_d$ controller.

For the next simulations of the system with control law, Eq.(19), we added piezoelectric actuators and sensors. We first obtained the locations and sizing of the actuators solving the problem of objective function minimization Eq.(32) using *Matlab* software. Figure 7 show the objective function that depends on l_a and x_a variables with $\alpha = 300$. The minimal value is obtained at $x_a = 0.09m$ and $l_a = 0{,}39m$ that represents the position and sizing of piezoelectric actuator bonded on flexible link.

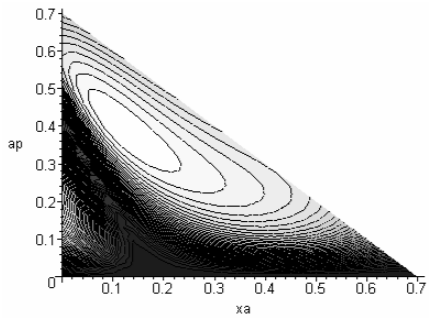

Figure 7. Energies dissipated objective function due to piezoelectric control action.

Figure 8 (b) shows a reduction on the frequency and deflection amplitude induced by the tracking control when piezoelectric actuators and sensors are added.

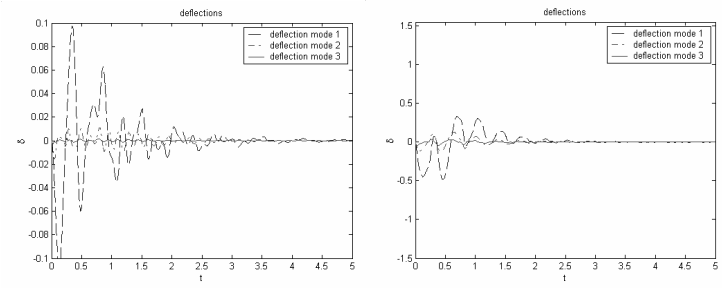

(a) *(b)*

Figure 8. (a) Deflections of first, second and third modes for damping system with robust control.
(b) Deflections of first, second and third modes for damping system with piezoelectric actuator and sensor.

Figure 9 (a) and (b) also shows a reduction on the trajectory tracking error control when piezoelectric actuators and sensors are added.

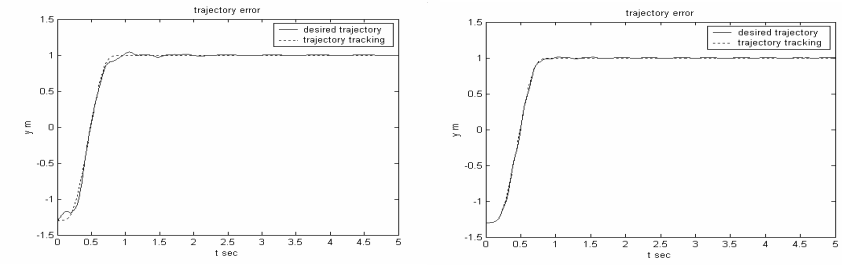

(a) *(b)*

Figure 9. (a) Vertical trajectory error with robust control.(b) Vertical trajectory error with piezoelectric actuator and sensor.

Figure 10 (a) and (b) shows a reduction on the frequency and deflection amplitude, in the first mode, induced by the tracking control when piezoelectric actuators and sensors are added.

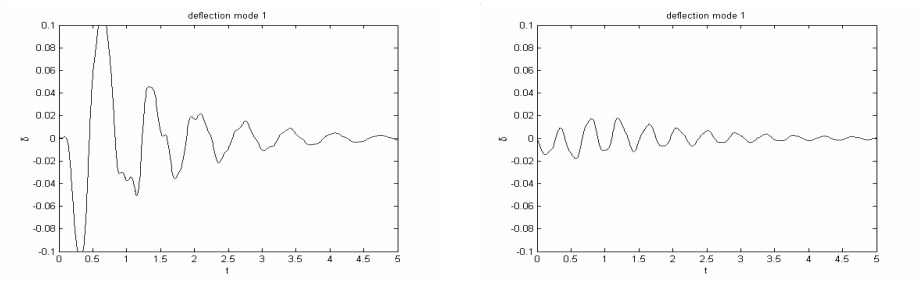

(a) *(b)*

Figure 10. (a) Deflections of first mode for damping system with robust control. (b) Deflections of first mode for damping system with piezoelectric actuator and sensor.

Figure 11 (a) and (b) shows a reduction on the frequency and deflection amplitude, in the second mode, induced by the tracking control when piezoelectric actuators and sensors are added.

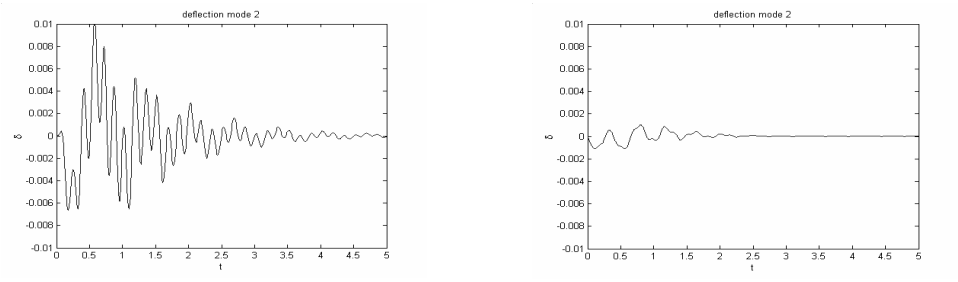

(a) *(b)*

Figure 11. (a) Deflections of second mode for damping system with robust control. (b) Deflections of second mode for damping system with piezoelectric actuator and sensor.

Figure 12 (a) and (b) shows a reduction on the frequency and deflection amplitude, in the third mode, induced by the tracking control when piezoelectric actuators and sensors are added.

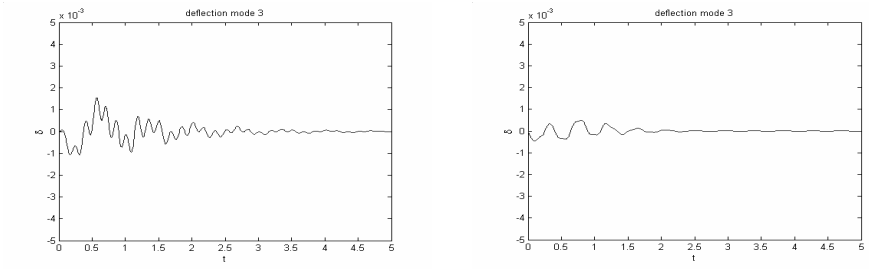

(a) *(b)*

Figure 12. (a) Deflections of third mode for damping system with robust control.
(b) Deflections of third mode for damping system with piezoelectric actuator and sensor.

It is clearly seen in Figures 8, 9, 10, 11 and 12 that the frequency and deflection amplitude is reduced by activating the piezoelectric actuators and sensors during the motion.

12. Conclusions and considerations

In this work we introduced a technique for tracking and vibration control of a robot with flexible links. This technique uses the motor torque for the joint angle control and also for control the low frequency vibrations in the robot links. Piezoelectric actuators and sensors are added to the system to control the high frequency vibrations that cannot be reduced by the motor alone. We also introduced an optimization procedure for the size and position of the piezoelectric actuator and sensor, using the energy dissipated by the control in the objective function. This technique can be developed to build light manipulators with flexible links, while preserving the force and precision. It also reduces the energy consumption and suits the needs for aerospace systems or for tasks that demand lightness, precision and agility.

For geometric complex links, the eigenvectors are approximated using polynomial interpolation spanning all finite elements of each flexible link. The Rayleigh quotient was used for the validity of the technique. Hermite polynomials proved to be the best approximation for this case.

13. References

1. V. Bottega, R. Pergher, A. Molter and J. S. O. Fonseca, "Modelagem, controle e simulação de manipuladores robóticos com braços flexíveis de geometria irregular". In: CMNE/CILAMCE Iberian Latin American Congress on Computational Methods in Engineering, Porto, 2007.

2. S. Arimoto, *Control Theory of Non-Linear Mechanical Systems*, Oxford Clarendon Press, London, 1996.

3. J. K. Bathe and E. L. Wilson**,** *Numerical Methods in Finite Element Analysis*. Prentice Hall, 1976.

4. D. L. Clive and I. H. Shames, *Solid Mechanics. A variational approach*, McGraw-Hill, 1973.

5. V. Bottega. "Controle de sistemas mecânicos não-lineares aplicado a um manipulador robótico", Dissertação de Mestrado, UFRGS/CPGMAP, Porto Alegre, 1998.

6. W. J. Book, "Recursive lagrangian dynamics of flexible manipulator arms", Int. Journal Robotics Res., vol. 3, no. 3, pp. 87-101, 1984.

7. Meirovitch, *Analytical Methods in Vibration*, Macmillan, New York, 1967.

8. A. de Luca, P. Lucibello and F. Nicolo, "Automatic symbolic modeling and nonlinear control of robots with flexible links". In Proc. IEEE Work on Robot Control, Oxford, UK, pp. 62-70, 1988.

9. D. Luenberger, "Algorithmic analysis in constrained optimization". SIAM-AMS Proceedings, 9, pp.39-51, 1976 .

10. M. A. Arteaga, "On the properties of a dynamic model of flexible robot manipulators", ASME Journal of Dynamics Systems, Mesurement, and control, vol. 120, pp. 8-14, 1998.

11. J. P. La Salle and S. Lefschetz, " Stability by Lyapunov's direct method", Academic Press, New York, 1961.

12. E. F. Crawley and J. De Luis, "Use of piezoelectric actuators as elements of intelligent structures", AIAA Journal, vol. 25, pp. 1373-1385, 1987.

13. H. T. Banks, R. C. Smith and Y. Wang, *Smart material structures: modeling, estimation and control*, John Wiley & Sons, Paris, 1996.

14. Denoyer, K. K. and Kwak, M. K., 1996, "Dynamic Modelling and Vibration Suppression of a Slewing Structure Utilizing Piezoeletric Sensor and Actuators", Journal of Sound and Vibration, vol. 189, no. 1, pp. 13-31.

15. Li, Y., Onoda, J. e Minesugi, K., 2002, "Simultaneous Optimization of Piezoelectric Actuator Placement and Feedback for Vibration Suppression", Acta Astronautica, vol. 56, no. 6, pp. 335-341.

16. De Luca, A., Lucibello, P. and Nicolo, F., 1988, "Automatic Symbolic Modeling and Nonlinear Control of Robots with Flexible Links". In Proc. IEEE Work on Robot Control, Oxford, UK, pp. 62-70.

17. V. Bottega, "Controle e otimização estrutural de manipuladores robóticos com elementos flexíveis usando atuadores e sensores piezelétricos". Tese de Doutorado, UFRGS/CPGMAP, Porto Alegre, 2005.

18. A. de Luca, L. Lanari S. Lucibello and Panzoeri, "Control experiments on a two-link robot with a flexible forearm", 29th IEEE Conf. Decision and Control, Honolulu, HI, pp 5-7, 1990.

19. S. B. Cho, S. S. Cho, H. C. Shin and H. K. Kim, "Quantitative feedback theory control of a single-link flexible manipulator featuring piezoelectric actuator and sensor", Smart Material Structures, vol. 8, pp. 338–349, 1999.